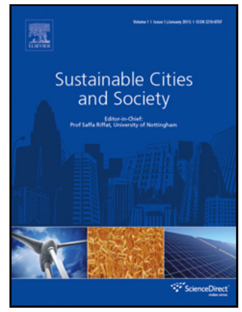

Title: Mapping the energy flexibility potential of single buildings equipped with optimally-controlled heat pump, gas boilers and thermal storage

Author: Francesco D'Ettorre Mattia De Rosa Paolo Conti Daniele Testi Donal Finn

PII: S2210-6707(18)32678-7
DOI: https://doi.org/doi:10.1016/j.scs.2019.101689
Reference: SCS 101689

To appear in:

Received date: 24 December 2018
Revised date: 14 June 2019
Accepted date: 26 June 2019

Mapping the energy flexibility potential of single buildings equipped with optimally-controlled heat pump, gas boilers and thermal storage

Abstract

The present paper assesses the capability of a cost-optimal control strategy to activate demand response actions in a building equipped with an air-source heat pump coupled with a water thermal storage system. Commencing with a reference scenario where no demand response actions are considered, the electricity consumption pattern and the operational cost are evaluated. Several demand response scenarios are next considered by adapting consumption patterns by reduction of baseline heat pump power consumption. The difference between the operational cost evaluated under a specific demand response program and the benchmark cost are used to assess the marginal cost that should be considered to provide incentives to promote user participation in demand response programs. The results illustrate the effectiveness of thermal energy storage for reducing the total system operational cost and its seasonal primary energy consumption, both with and without demand response actions. The application of the proposed methodology over the whole heating season, allows performance maps to be created that can be used either by the grid-operator or end-user to identify the best demand response action to be implemented on any particular day. These maps represent useful decision tools to assess and optimise the flexibility potential while meeting end-user needs.

Keywords: energy flexibility, building, smart grids, thermal storage, heat pump, model predictive control

1. Introduction and state of the art

One of the main objectives of the EU's energy policies is the reduction of greenhouse gas emissions by 80-95% by 2050 [1]. This decarbonisation process requires policies promoting investment in new low-carbon technologies, energy efficiency measures, renewable energies and grid infrastructure. Reaching high penetration of Renewable Energy Sources (RES) is widely recognised as one of the first steps towards the development of new energy systems capable of meeting EU targets, while increasing competitiveness and supply security. Notwithstanding, the experiences from countries with high shares of RES - such as Denmark, where renewable electricity generation accounts for approximately two thirds of the overall production [2] - have highlighted challenges related to the technical integration of RES into the existing power system network.

Since the power grid requires a continuous match between power supply and demand, the intrinsic stochastic nature of renewable sources makes this balance challenging [3]. Moreover, even if the traditional power system is capable of coping with uncertainty in both demand and supply power profiles, the flexibility offered by the supply-side might not be sufficient compared to the flexibility required for high penetration of RES. Therefore, in order to increase the RES share, and to use energy more effectively, energy system flexibility needs to be improved. Alongside traditional measures, i.e., supply-side regulation and power grid upgrades, new flexibility sources can be obtained by enabling the active participation of the demand-side in the power system operational procedures.

Generally, the term *demand side management* (DSM) refers to the modification of end user demand by implementing strategies capable of reducing end user energy consumption, harnessing demand efficiencies, improved control and optimisation as well as incorporating RES measures. Among these solutions [4], demand response (DR) strategies are gaining increased attention as promising techniques for the emerging smart grid by providing better integration and exploitation of renewable energy sources, through the management of end user generation and consumption patterns. DR has been shown to be a promising proposition [5] and is based on adapting user demand profiles to grid requirements, by increasing, reducing, or shifting the amount of energy consumed, according to external signals coming from the grid operator (e.g., electricity prices). DR programs can be classified either as (for an exhaustive description of the different DR programs, refer to [6]):

- Incentive-Based Programs (IBP): consumers receive incentive payments in return for the load-reduction provided over a given period. Programs belonging to this category can be classified as Direct Load Control, Curtailable Load and Demand Bidding.

- Price-Based Programs (PBP): consumers voluntarily schedule their consumption profiles according to economic signals, such as electricity tariffs. PBP can be classified according to dynamic pricing rates, i.e., time-of-use tariff, critical peak and real-time pricing.

This classification leads to another interesting aspect related to the type of DR followed by the *prosumer*, which can be either active or passive depending on the type of program adopted. Typically, IBPs lead to active DR actions, since prosumers change their consumption patterns (DR) following specific requests from the grid. These DR actions can drive the system to sub-optimal working conditions (either from a technical and economic point of view), leading to higher operational costs and consequently to positive marginal costs of the flexibility provided. Hence, incentives are needed to promote the involvement of the consumers in these kind of programs. On the other hand, PBPs encompasses passive DR behaviour, since consumers adapt their consumption profiles to the electricity price patterns, with the aim of minimising operational costs. Even if the tariff structure leads the consumers to decrease their consumption during peak hours, providing an indirect service to the grid (i.e., passive), no active interactions between these actors are in place. End-user ability to control the demand in response to electrical grid requirements strictly depends on their type and size. Industrial consumers can play a more significant role due to the magnitude of their energy and power demands. Moreover, they are often readily equipped with the facilities required to implement energy management and DR measures, even if their potential has not yet been fully and thoroughly exploited [7, 8].

Besides industrial users, residential and commercial end-users are potential providers of demand response, since the building sector accounts for about 40% of the primary energy consumption worldwide [9]. In Europe, heating and cooling loads in residential and commercial buildings account for almost 50% of the total final energy demand, being responsible for about 36% of all GHGs emissions [10]. Consequently, the decarbonisation of the heating sector must be addressed to successfully complete the transition towards a more sustainable, secure and affordable energy future. To this aim, the EU has developed several directives aimed at improving the energy performance of buildings. Among these, the Energy Performance of Building Directive (EPBD) [11] and the Energy Efficiency Directive (EED) [12] are the main legislative instruments established to promote long-term strategies for mobilising efforts aimed at implementing energy efficiency measures and at fostering active participation of end-users in the energy market. Moreover, the EBPD directive was recently updated (EPBD Directive 2018/844/EU [13]) by introducing instruments to support the use of smart technologies and technical building systems through the establishment of a Smart Readiness Indicator (SRI). This indicator will allow for the rating of the smart readiness of buildings, i.e., the capability of buildings (or building units) to adapt their operation to the needs of occupants and to signals from the grid (energy flexibility) [14].

Among the different technologies available for implementing demand response actions, the use of advanced control strategies for the management of electric heat pumps and thermal energy storage is one promising solution [15–21]. In this context, defining the flexibility potential is not a straightforward process due to the absence of common accepted definitions, quantification methodologies and standardised assessment procedures [22–24].

Stafford [25] defined the flexibility potential of two hybrid heat pump/gas boiler systems as the percentage of the building load which can be shifted from the heat pump to the gas boiler in response to grid requirements (switching off the heat pump for approximately 1 hour at periods of peak consumption). The results showed that the load share between the two generators can be shifted towards the gas boiler with only a modest increase in the overall energy consumption. A methodology to assess the resulting energy penalty using the heat pump thermal output as a predictor of system energy consumption was outlined, but economic assessment was not considered.

Similarly, Oldewurtel et al. [26] developed a methodology to quantify the energy shifting potential of different buildings by using a model predictive control (MPC) and predefined price signals. The flexibility potential was characterised by means of an efficiency parameter defined as the ratio between the maximum power shift and the resulting additional energy consumption of the system, while there was no explicit mention of resulting additional costs. An analogous methodology was presented by De Coninck et al. [27], who defined the building flexibility as the maximum positive (and negative) deviations from a reference cost-optimal consumption pattern available during a given time period of the day. An existing office building equipped with electrically-driven air source heat pumps and gas boilers were used as a case study: three optimal control problems were solved to determine a cost-optimal baseline for the consumer, and then the maximum positive and negative flexibility over the DR action interval (from one to three hours) was examined while maintaining the building indoor temperature within the comfort boundaries.

Ali et al. [28] proposed a hierarchical two-stage optimisation framework for a residential building: at first, a cost-optimal consumption profile is defined on the basis of the hourly prices of the day-ahead market; then, a second stage is set up where incentives are provided to customers if they either increase or reduce their hourly consumption patterns. Adopting similar assumptions, Bianchini et al. [29] considered a DR strategy based on external pricevolume signals sent by an aggregator to the building energy management system. A model predictive control strategy was adopted to minimise the energy cost, while a heuristic algorithm based on problem decomposition was developed to reduce the computational cost.

Although the above mentioned works outline the lack of a commonly adopted methodology, it is worth mentioning the work of IEA Annex 67 in establishing standardised and harmonised procedures to characterise energy flexibility of individual buildings and building clusters [30]. To this end, the IEA EBC Annex 67 has identified initially the dimensions of energy flexibility, namely capacity, duration and cost. Then, the energy flexibility potential is evaluated by determining the capability of buildings and systems to change associated energy demand profiles, with respect to a reference scenario, according to external penalty signals (e.g., energy prices, carbon dioxide emissions, RES exploitation, etc.), acting as additional boundary conditions [31]. Once the dynamic response of a building (or cluster of buildings) to the penalty signal is identified, each flexibility dimension is then assessed by evaluating its deviation from the reference value (e.g., the relative amount of saved carbon dioxide emissions).

While many authors have focused on the optimal control of integrated hybrid systems to implement DSM [32–35], quantitative technical, economic and environmental assessments of the energy flexibility associated with hybrid systems (gas boiler/heat pump/thermal storage) are still scarce. Research efforts are still required in order to address the research needs in terms of data, modelling approaches and assessment methodologies, as highlighted by Kreuder and Spataru [36]. Moreover, developing such methodologies is paramount for establishing policies and business opportunities leading towards a more rational and sustainable use of energy in cities. Compounding this research gap, is the lack of common definitions and standardised procedures to determine the *flexibility cost*, as well as the provision of exhaustive and comprehensive generalisations capable to extending information at larger scale and to establish appropriate policy and legislation frameworks [37]. In this context, the techno-economic and environmental assessment of the flexibility potential offered by hybrid heat pump-gas boiler generators has to date been rarely investigated. Therefore, the present paper focuses on:

- proposing a set of comprehensive indicators capable of assessing the performance of DR programs and to identify DR actions which fit a specific user requirements,
- presenting a methodology to develop a control algorithm for hybrid heat pump, in this case boiler systems aimed at minimising the daily operational costs and enabling the implementation of DR programs,

- investigating and assessing different DR programs from a techno-economic and environmental point of view, by creating performance decision-making maps for end-users, building managers and grid network operators.

To this purpose, an optimal control problem (OCP) is solved to determine the control strategy of the thermal generators and the storage tank, to meet the load at minimum cost. In addition, the impact of a price-based DR program is investigated in terms of consumption patterns and daily operational costs. Different scenarios in terms of requested flexibility from the grid under IBPs are investigated to determine associated operational costs. Since any deviation from the optimal control strategy obtained by solving the OCP will result in sub-optimal operation, leading to higher operating costs, the difference between the new operational costs and the benchmark cost relating to the PBP is used to assess the minimum pay-out that should be adopted in an IBP scenario to promote the involvement of the consumer in this kind of program.

The following structure is adopted in the paper: Section 2 describes the methodology used to assess the cost associated with different DR actions, the system modelling and the optimal control problem formulation. Section 3 presents a description of the case study analysed and Section 4 discusses the results obtained. Finally, Section 5 summarises the main findings of the work.

2. Methodology

2.1. System overview and modelling

A building equipped with a hybrid generator composed of an electrically-driven air-source heat pump, coupled with a gas boiler, was assumed as a case study, as outlined in Figure 2. The generators are considered to be operating in parallel: when the heat pump cannot meet the required thermal output, the boiler supplies the residual load demand. Both generators are controlled by a model predictive control (MPC) strategy. Unlike traditional controller, model predictive control is an advanced method of control which, compared to more traditional controller, is capable to evaluate the best control actions ($\mathbf{u}$) to be implemented not only on the basis of the current state of the system, but also based on information (predictions) about future disturbances ($\mathbf{w}$) that can affect the behaviour of the system. At each time-step t, the control action is evaluated solving an open loop optimal control problem, whose aim is to minimise over a finite prediction horizon τ a specific objective function J (e.g. total cost or CO_2 emissions). Once the OCP is solved, the controller implements the optimal control trajectory ($\mathbf{u}_{opt}$) over the control horizon only, i.e., a 1 hour time step. A schematic view of the MPC procedure is given in Figure **??**.

Two different system configurations are considered: the first one (Figure 2a) consists of the hybrid generator only, whereas the second one (Figure 2b) includes also a space heating water tank connected in series to the heat pump to decouple the energy generation and distribution. The TES is considered for space heating only. Although combining a TES with an existing DHW tank can be considered as a further option, the adoption of two separated tanks is generally preferable, as shown in [18, 38–40]. First, space heating tanks

for $t = 1$ **to** $\mathcal{H}$ **do** `// e.g., for each hour of the heating season`

STAGE 1: Get information about future events

Forecast disturbances over the prediction horizon τ: `// e.g. external temperatures or electricity prices;`

$\mathbf{w}_j = [w_j^{t|t}, w_j^{t|t+1}, \ldots, w_j^{t|t+i}, \ldots, w_j^{t|t+\tau-1}]\ \forall j \in [1, \mathcal{N}]$

with $w_j^{t|t+i}$ the value of the j-th disturbance at time steps $t+i$ as predicted at time step t and $\mathcal{N}$ the number of disturbances.

STAGE 2: Solve the open loop optimal control problem

Identify the control sequence $\mathbf{u}_{opt}$ that minimise the objective function J over the considered horizon τ:

$\mathbf{u}_{opt} = \underset{\mathbf{u}}{\operatorname{argmin}}\ J(\mathbf{u}, \mathbf{w}) = \underset{\mathbf{u}}{\operatorname{argmin}} \sum_{l=0}^{\tau-1} f(\mathbf{u}^{t|t+l}, \mathbf{w}^{t|t+l})$

where:

$\mathbf{w}^{t|t+l} = [w_1^{t|t+l}, w_2^{t|t+l}, \ldots, w_j^{t|t+l}, \ldots, w_{\mathcal{N}}^{t|t+l}]$

$\mathbf{u}^{t|t+l} = [u_1^{t|t+l}, u_2^{t|t+l}, \ldots, u_k^{t|t+l}, \ldots, u_{\mathcal{M}}^{t|t+l}]$ `//` $\mathcal{M}$ `number of control variables;`

output: Optimal trajectories

$\mathbf{u}_{opt,k} = [u_k^{t|t}, u_k^{t|t+1}, \ldots, u_k^{t|t+i}, \ldots, u_k^{t|t+\tau-1}]\ \forall k \in [1, \mathcal{M}]$

STAGE 3: Implementation

Once the optimal control trajectories are known then only their first elements are implemented by the controller by setting:

$\mathbf{u} = [\mathbf{u}_{opt,1}^{t|t}, \mathbf{u}_{opt,2}^{t|t}, \ldots, \mathbf{u}_{opt,k}^{t|t}, \ldots, \mathbf{u}_{opt,\mathcal{M}}^{t|t}]$

then move to the next time step.

end

Figure 1: MPC algorithm

are characterised by higher capacities, due to the higher energy demand required for heating than for DHW [18]. Moreover, DHW demand is intrinsically stochastic, since it follows consumer needs, and it needs to meet specific quality standards for health reasons (i.e., by performing anti-legionella cycles). All these aspects make the use of space thermal energy storage (TES) tanks more suitable for implementing DR measures.

The boiler is considered connected directly to the thermal load in both the configurations. The performance of different kinds of electrically–driven heat pump units can show different behaviour depending on the unit control strategy [41]: during part–load operations, an on-off unit modulates its capacity by varying its sequence of on-off cycles, while a modulating unit can work continuously by reducing its thermal power and, consequently, the energy delivered. Therefore, when the part-load factor is reduced, the coefficient of performance (COP) decreases for on–off units, while for modulating units it remains constant until a minimum part–load factor is achieved [42].

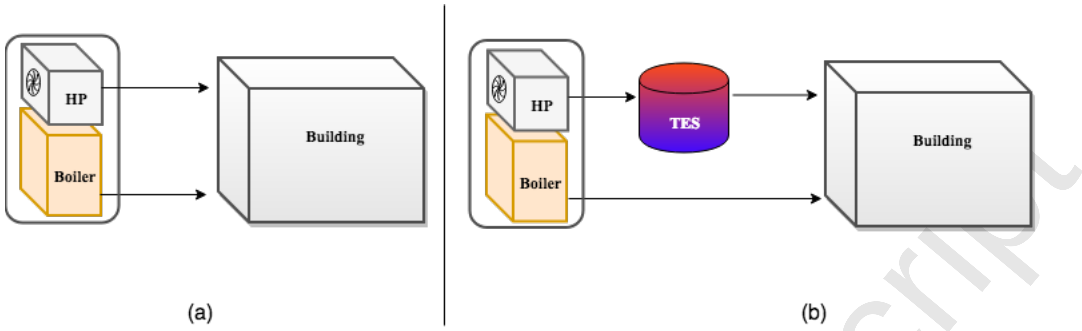

Figure 2: Schematic of the heating system (a) without and (b) with TES.

Generally, the coefficient of performance of a heat pump at full load conditions (COP_{FL}) can be evaluated by means of the so-called second law efficiency η^{II}, as shown in Eq. 1:

$$COP_{FL} = \eta^{II} \cdot COP_{Carnot} = \eta^{II} \cdot \frac{T_H + 273.15}{T_H - T_L} \tag{1}$$

where COP_{Carnot} is the coefficient of performance of a Carnot cycle operating between a high temperature (T_H) and a low temperature (T_L) reservoirs – i.e., the condenser and evaporator temperatures. To take into account the variation of the heat pump performance with the load-factor, a part-load correction factor (f_{PL}) is introduced according the standards EN 14825 [43] and UNI/TS 11300–4 [44]:

$$f_{PL} = \frac{CR}{(1 - C_c) + C_c CR} \tag{2}$$

The term C_c in Eq. 2 represents the degradation coefficient, assumed to be equal to 0.9, as suggested in [43, 44], while CR is the heat pump part-load ratio, defined as the ratio between the delivered thermal power ($\dot{Q}_{HP,th}$) and the heat pump maximum power ($\dot{Q}^{max}_{HP,th}$), as shown in Eq. 3.

$$CR = \frac{\dot{Q}_{HP,th}}{\dot{Q}^{max}_{HP,th}} \tag{3}$$

The COP over all of the operative range can be expressed as shown in Eq. 4.

$$COP = \eta^{II} \cdot COP_{Carnot}(T_L, T_H) \cdot f_{PL}(CR) \tag{4}$$

Moreover, the heat pump can operate only if the external temperature is higher than a cut-off value ($T_{ext} > T_{cut-off}$), otherwise it is switched-off. Furthermore, in order to avoid comfort constraint violations, the gas boiler is designed to deliver all of the thermal power required by the load at any time, at a constant efficiency η_B over all operative ranges. The thermal energy storage is modelled as a perfectly mixed water tank, the temperature T_{TES} of which varies according the following energy balance:

$$V_{TES}\rho_w c_w \frac{dT_{TES}(t)}{dt} = \dot{Q}_{HP,th}(t) - \dot{Q}_{TES,th}(t) - \dot{Q}_{TES,loss}(t) \tag{5}$$

with V_{TES} the volume of the storage tank and ρ_w and c_w the density and the specific heat capacity of water, respectively, while $\dot{Q}_{TES,th}$ is the power delivered by the storage to the load. When optimising a heating/cooling system coupled with a TES, the most common approach is to model the storage energy content as a single state, i.e., perfectly mixed [45–47]. This assumption allows to simplify the optimal control problem formulation, which otherwise would result in a non-convex optimisation problem. Moreover, incorporating buoyancy or mixing would result in transient model behaviour and, consequently, unsuitable for gradient based optimization methods, as outlined in Beaten et al. [48]. Furthermore, the assumption of perfect mixing represents a conservative hypothesis, since neglecting the spatial distribution of the temperature profile in the tank leads to a lower exploitation of the TES, since the storage is not used to its full extent, as it has been shown in [48].

The storage losses ($\dot{Q}_{TES,loss}$) are evaluated as shown in Eq. 6, where UA_{TES} is the overall heat transfer coefficient, considered proportional to the size of the tank [49], while $\Delta T(t)$ is the difference between the storage temperature and its surrounding temperature.

$$\dot{Q}_{TES,loss}(t) = UA_{TES} \cdot \Delta T(t) \tag{6}$$

Finally, Eq. 7 is used to determine the useful stored energy a state of charge (SoC) parameter, in which T_{em} and T_{TES}^{max} are the constant temperature required by the emission system and the maximum storage temperature, respectively.

$$SoC = \frac{T_{TES} - T_{em}}{T_{TES}^{max} - T_{em}} \tag{7}$$

2.2. OCP and implementation of DR program

2.2.1. Baseline OCP

In order to define a baseline case to assess the impact of the applied active demand response measures, a scenario with no DR measures is considered. In this scenario, the hybrid generator is controlled by an MPC strategy aimed at satisfying the load demand while minimising the operative-cost of the system, according to the hourly profile of the electricity tariff from the day-ahead market. To this end, an open-loop OCP is solved at each time-step over a chosen prediction horizon τ. Once the optimal control profiles are obtained, only the first action of the computed control sequence is implemented to get a new system state before the optimisation process is repeated. Since the OCP is aimed at minimising the operational costs for heating, the objective function J is defined as the cost over the horizon τ (C_τ), as shown in Eq. 8.

$$J = C_\tau = \int_0^\tau \left[p_{el}(t) \frac{\dot{Q}_{HP,th}(t)}{COP(t)} + p_{gas} \frac{\dot{Q}_{B,th}(t)}{\eta_B} \right] dt \tag{8}$$

$\dot{Q}_{HP,th}$ and $\dot{Q}_{B,th}$ in Eq. 8 are the thermal power delivered by the heat pump and the boiler, respectively, while p_{el} and p_{gas} denote the electricity and gas tariffs, respectively. The thermal dynamics of the storage tank ~~are~~ is considered as a state constraint expressed by the energy balance shown in Eq. 5. Several constraints must be applied to the operative ranges of the generators and the thermal energy storage. Regarding the generators, the following expressions are used:

$$\dot{Q}_{HP,th}^{min} \leq \dot{Q}_{HP,th}(t) \leq \dot{Q}_{HP,th}^{max} \quad \forall t \in [0, \tau] \tag{9}$$

$$\dot{Q}_{B,th}^{min} \leq \dot{Q}_{B,th}(t) \leq \dot{Q}_{B,th}^{max} \quad \forall t \in [0, \tau] \tag{10}$$

Moreover, information about the minimum temperature required by the building emitter system must be provided, since it affects the amount of useful stored energy. For this reason, and considering that the storage temperature (T_{TES}) varies during the day depending on the different charging and discharging phases (and heat losses), the storage is considered capable of delivering energy to the load only if its temperature is above the minimum temperature required by the emitter system. Considering $\dot{Q}_{S,th}$ as the power delivered by the storage tank to the building, this condition can be introduced as follows:

$$\begin{cases} \dot{Q}_{TES,th}(t) \geq 0, & if \;\; T_{TES}(t) \geq T_{em} \\ \dot{Q}_{TES,th}(t) = 0, & otherwise \end{cases} \quad \forall t \in [0, \tau] \tag{11}$$

Further constraints on the operative range of the storage tank temperature are introduced by means of the following inequalities:

$$T_{TES}^{min} \leq T_{TES}(t) \leq T_{TES}^{max} \quad \forall t \in [0, \tau] \tag{12}$$

In order to ensure the fulfilment of the building thermal demand at any time, the following constraint is added:

$$\dot{Q}_{TES,th}(t) + \dot{Q}_{B,th}(t) = \dot{Q}_{L,th}(t) \quad \forall t \in [0, \tau] \tag{13}$$

The implementation of the above methodology in a real control application requires the use of forecasting models for estimating future weather and market price profiles, which may affect the solution of the optimisation problem described above. As for instance, Felten and Weber [50] analysed the impact of forecast errors on estimating the flexibility potential of an air-source heat pump, coupled with a thermal heat storage and controlled by a MPC strategy. The results estimated differences of heat pump energy consumption and operation costs were below 5% when compared to the ideal case of a perfect foresight. Moreover, the authors showed that the effect of this error has to be considered as relevant when large storage are installed (i.e., $TES > 1\ m^3$). However, since the present work performs an *ex-post* analysis, in which historical weather and market price data are used as external signals, the assumption of a perfect forecast is considered.

2.2.2. DR strategy

Once the baseline OCP is solved, several active DR measures are implemented to adapt the user demand profiles to possible grid requirements. Indeed, depending on the specific circumstances - e.g. mismatch between power supply and demand - the amount of energy consumed can be increased (positive flexibility) or reduced (negative flexibility) by modifying the baseline heat pump electrical load profile ($P_{HP,el}^{ref}$). In view of this, the hourly electricity price is assumed to be an external signal driving the DR request from the grid end a threshold cost function has been introduced to simulate the activation of this condition which is, by definition, a discrete variable: DR request on or off [5, 51]. When the price is above the threshold value (p_{el}^{thld}), a DR action is activated, and the reference heat pump electrical power is reduced to a fraction (α) of its value, as shown in Figure 3. It is important to state that the identification of a methodology aimed at defining such a threshold price still represents a research gap, as highlighted by [5]. While fixed values over the whole year are widely adopted, as in [5], Rodriguez et al. [51] demonstrated that using dynamic thresholds, calculated on a daily basis and capable of capturing the daily price variations, represents a better alternative. Therefore, in the present work, the threshold price is evaluated by using the formulation adopted in [5] (Eq. 14), which is computed on a daily basis. The terms $\mu_{p_{el}}$ and $\sigma_{p_{el}}$ are the mean and the standard deviation of the daily electricity price profile, respectively.

$$p_{el}^{thld} = \mu_{p_{el}} + \sigma_{p_{el}} \tag{14}$$

Moreover, it is important to highlight that the adoption of a threshold value as a triggering signal for the activation of a DR action, does not affect the possibility to have an appropriate heat pump response. Arising from its predictive capability, the controller can schedule the heat pump operation taking into account any future DR requests, while evaluating its impact on the considered objective function, namely the operational costs of the system. In the present analysis, a maximum duration of the demand response action of two hours is considered [16]. Therefore, the baseline consumption profile is modified in a new target profile ($P_{HP,el}^{target}$) and a new OCP can be formulated by adding a flexibility constraint (Eq. 15) aimed at equalling the heat pump consumption profile with the target profile, during those hours in which the DR action is active ($\delta = 1$).

$$\int_0^\tau \left[\frac{\dot{Q}_{HP,th}(t)}{COP(t)} - P_{HP,el}^{target}(t)\right]^2 dt = 0 \tag{15}$$

$$P_{HP,el}^{target}(t) = \alpha \cdot \delta(t) \cdot P_{HP,el}^{ref}(t) \tag{16}$$

The term δ in Eq. 16 is a binary variable equal to unity only when the DR is active:

$$\delta(t) = \begin{cases} 1 & if \quad p_{el}(t) \geq p_{el}^{thld} \\ 0 & otherwise \end{cases} \tag{17}$$

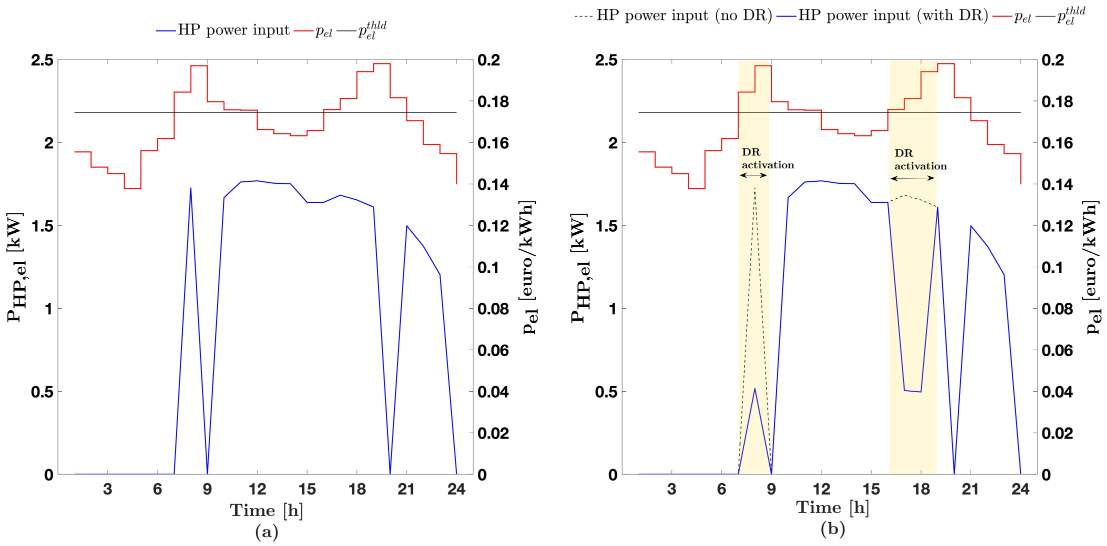

Figure 3: Demand Response measure.

2.2.3. *Flexibility indicators*

The impact of the applied demand response measures is assessed by comparing the daily costs resulting from the solution of the new OCPs and the reference costs. The cost-deviation from the baseline case can be defined as follows:

$$\delta C_{Flex} = C_{Daily}^{\alpha} - C_{Daily}^{ref} \tag{18}$$

while the marginal or specific cost can be defined as the ratio between cost-deviation (Eq. 18) and reduction in the heat pump electrical energy consumption due DR (δE_{DR}) as:

$$c = \frac{\delta C_{Flex}}{\delta E_{DR}} \tag{19}$$

An environmental indicator is also defined as the variation of the primary energy consumption caused by the DR actions (δPE):

$$\delta PE = PE_{DR} - PE^{ref} \tag{20}$$

3. Case Study

Since the current research investigates DR programs at the generator level (no DR actions at building level, e.g. changes in the internal temperature set point, are considered), the building is considered a boundary condition of the optimisation problem. To this end, a synthetic building thermal demand profile ($\dot{Q}_{L,th}$) is evaluated according to the Energy Signature method [52]. This method evaluates the building load demand as a linear function of the temperature difference between the indoor air and the external air, whose slope and intercept are indexes of the overall heat transfer coefficient and the maximum building thermal load, respectively.

Considering the internal air thermostatically controlled, the thermal load reaches the design value ($\dot{Q}_{L,th}^{max}$) when the external temperature reaches the design outdoor temperature (T_{ext}^{des}), while it becomes zero at the switch-off temperature (T_{ext}^{off}), where building gains and losses are balanced and the heating system is turned off (see Eq. 21).

$$\dot{Q}_{L,th} = \dot{Q}_{L,th}^{max} \cdot \left(1 - \frac{T_{ext} - T_{ext}^{des}}{T_{ext}^{off} - T_{ext}^{des}}\right) \tag{21}$$

The building is assumed to be located in North-Eastern Italy, in the city of Trieste, within the Italian climatic zone E [53]. The maximum required heating load of the buildin is 6 kW at a design temperature of $T_{ext}^{des} = -1.1\ ^oC$ and a room temperature of 20 ^oC, while it becomes equal to zero when the external temperature is $T_{ext}^{off} = 20\ ^oC$. The resulting thermal load profile obtained is shown in Figure 3a. The hourly profile of the external temperature (Figure 3b) was taken from the Italian Thermo-Technical Committee [54].

The COP of the HP is evaluated as described in Section 2.1 (Eq. 1 and Eq. 4) considering the temperature of the storage tank as T_H and the external temperature as T_L. The heat pump cut-off temperature is set equal to $T_{cut-off} = 0\ ^oC$ [55], while a low temperature heating emitter system with a constant emitter supply temperature (T_{em}) of 45 ^oC is considered [19, 42].

The storage tank, assumed to be located in a utility room with a constant temperature equal to ^oC, is sized such that the maximum heat load of the year can be supplied to the building for 2 hours [56]. Considering the allowed temperature difference in the storage $\Delta T_{TES} = 20\ ^oC$ and the specific heat capacity of water, this leads to a storage size of 0.086 m^3 per kW nominal heat load, which for a maximum building heating demand of 6 kW corresponds to a storage size of around 0.5 m^3.

Several demand response strategies are considered according to the procedure described in Section 2.2, on the basis of hourly values of the electricity prices extracted from the Italian Electricity Market Operator (EMO) database with regard of the year 2017 (Figure 3c) [57]. The threshold value for the activation of the DR action is determined in accordance with Eq. 14, while different DR measures are investigated by varying the term α, in the range [0.3,1]. Finally, the natural gas price is considered constant and equal to 0.08 €$/kWh$. All the simulations were performed over the heating season, which goes from the 15th October to the 15th April according to D.P.R n.412/1993 [53]. Table 1 summarise the characteristics of the building load demand and of the heating and emission systems.

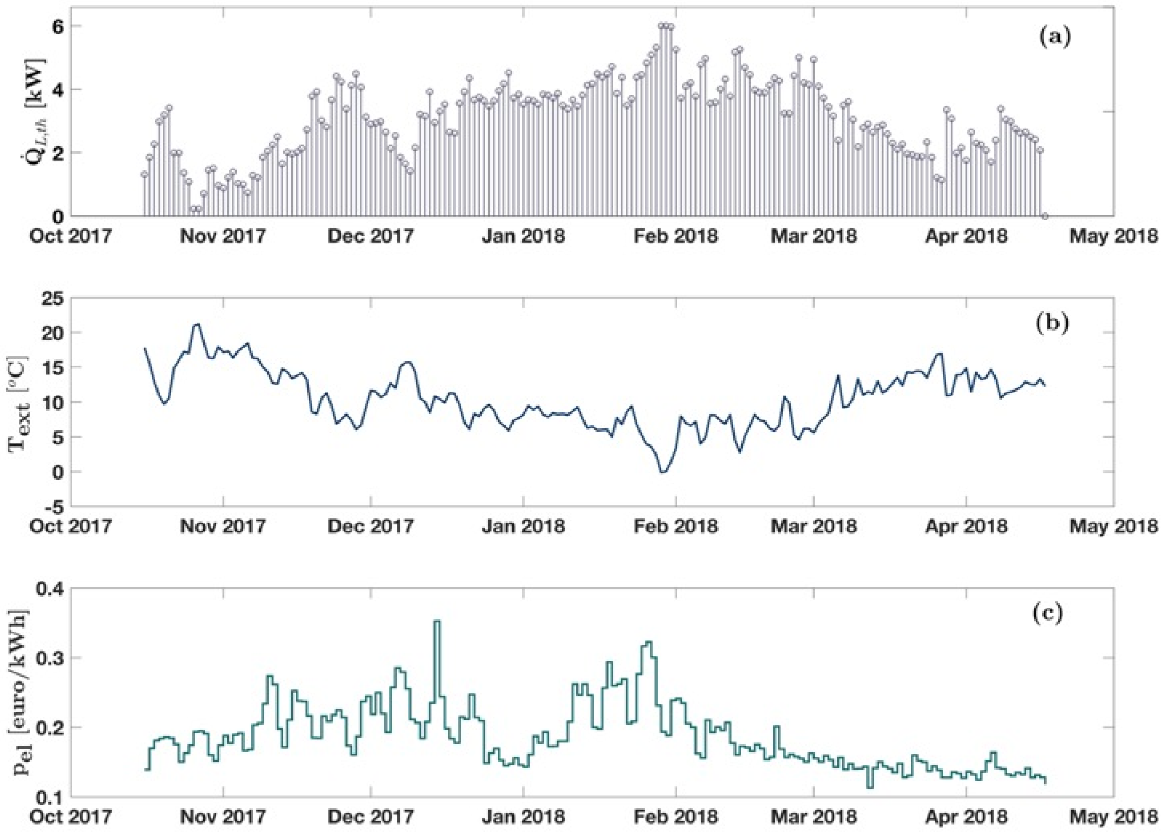

Figure 4: Hourly Profiles during the heating season: (a) Building heating demand; (b) External temperature; (c) Electricity prices.

Parameter	Units	Value
Annual energy consumption	kWh	7740
Peak load demand $\dot{Q}_{L,th}^{max}$	kW	6
Design external temperature T_{ext}^{des}	^oC	-1.1
Shut-off temperature T_{ext}^{off}	^oC	20
Emitter temperature set-point T_{em}	^oC	45
Heat pump size	kW	4
Boiler efficiency	-	0.96
TES size	m^3	0.5/0.75
U_{TES}	W/m^2K	0.5

Table 1: Characteristics of the building and its heating system.

The continuous form of the two OCPs, as described in Section 2.2, is converted into a non-linear programming problem (NLP) by using a direct collocation technique, with three collocation points for each simulation time step, which is set equal to 1 hour [58]. The resulting NLP is solved over a discretised prediction horizon of 24 hours using the CasADI interface to IPOPT with Python [59].

4. Results and discussion

Section 4.1 gives a flexibility assessment based on different hybrid system configurations. In particular, the impact of a TES on control strategy and resulting seasonal costs and energy consumption is compared to a configuration with no TES. In section 4.2, a characterisation of energy flexibility potential and associated marginal costs is presented with regard to the configuration with TES for different DR actions.

4.1. Impact of TES

Table 2 presents the results based on the methodology described in Section 2 and includes the baseline OCP problem with an implemented PBP for the configuration without TES and with TES. It can be observed a cost-saving and a reduction in seasonal primary energy consumption up to 8% and 13.5%, respectively, for the configuration with TES compared to that without a storage tank. Both results are due to the capability of the controller to exploit periods when low electricity tariffs apply. This can be observed by analysing in detail the daily operation of generators in both cases (see Figure 5).

Configuration	**Boiler share [%]**	**HP share [%]**	**PE [kWh]**	**Tot. Cost [€]**
no TES	49.5	50.5	7423	590
TES (0.5 m^3)	24.5	75.5	6444	541

Table 2: Seasonal load share, primary energy (PE) consumption and total cost for the configuration without and with TES under a PBP.

Figure 5 shows the daily operation of the generators (Figure 5a and 5b) over the first week of February (chosen as being representative of typical winter conditions) for both analysed configurations. In addition, the net energy balance of the TES is presented in Figure 5c. On the basis of Eq. 5, positive energy represents the charging phase of the tank (input greater than output), while negative energy the discharging phase.

Figure 5d, represent the evolution of the state of charge of TES over the considered period. It can be noted that without TES, the controller operates the heat pump for most of the time, while the gas boiler enters into production only during hours during which the electricity price reaches high values. On the other hand, if a TES is introduced, this behaviour is limited only to the 5th and 6th day of the week. This can be explained by comparing the thermal energy delivered by the boiler for the configuration without TES and its relationship with the maximum storage capacity (equal to 8 kWh). For this case, the thermal energy delivered by the boiler during days 1 to 4 is lower than the storage capacity and, consequently, the load shift operated by the controller to pre-charge the storage unit by running the HP during off-peak periods is enough to avoid the activation of the gas boiler during those hours when the HP is less cost-effective. On the other hand, for days 5 and 6,

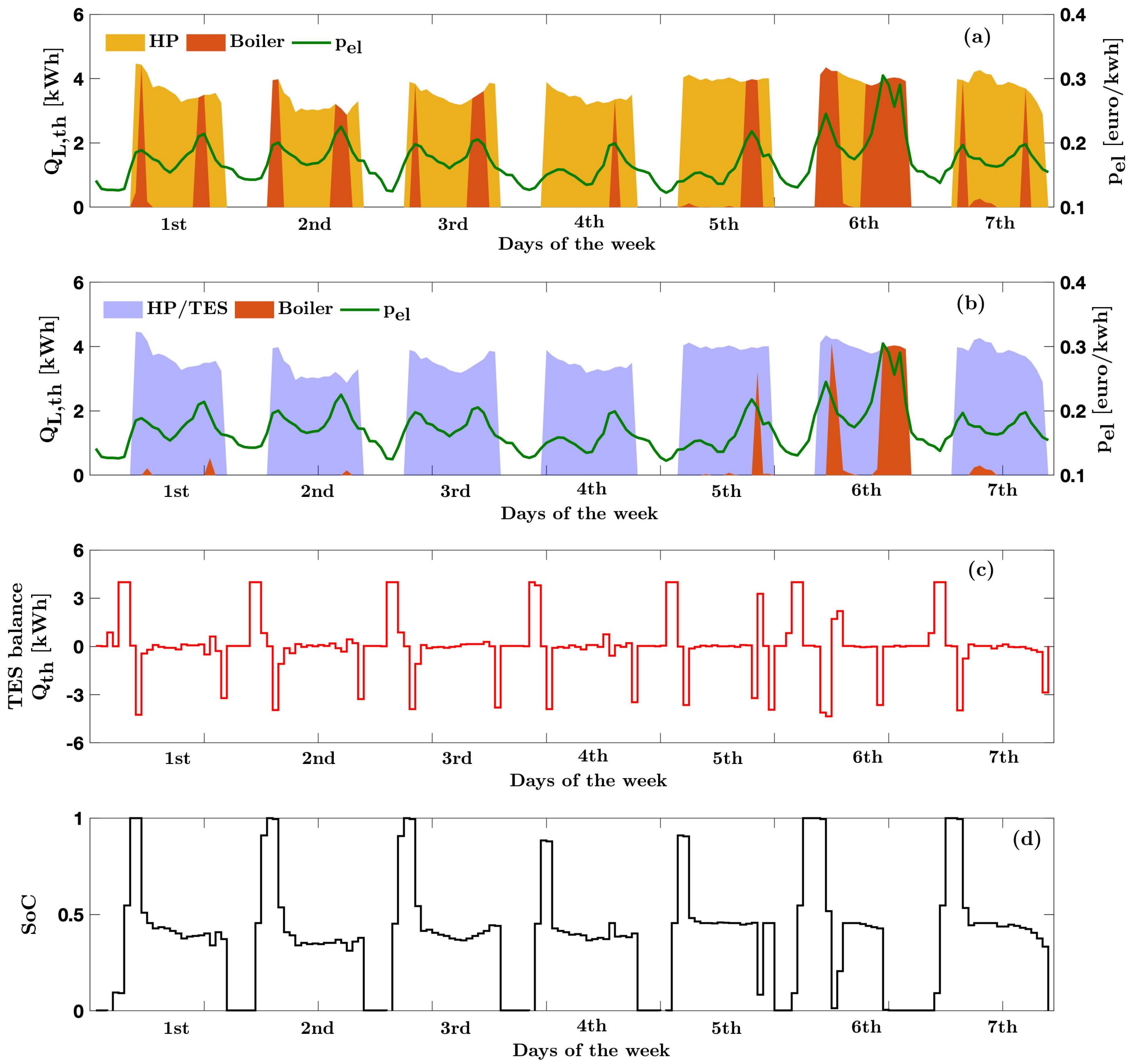

Figure 5: Hourly profile between February 1st and 7th: (a) Load share between heat pump and boiler (configuration without TES); (b) Load share between heat pump/TES and boiler (configuration with TES); (c) Charging and discharging phases of TES; (d) State of charge (SoC) of TES.

the TES is not capable of storing all the energy required to avoid the boiler entering into production.

To better understand the logic followed by the controller, Figures 6 and 7 examine in more detail the results obtained for day 2. In the configuration without TES, the control strategy prioritises the most cost-effective generator for each time step. In particular, it can be noted that the controller operates the HP only when its COP is higher than a threshold value (COP_{eq}), calculated on the basis of electricity and gas prices and the efficiency of the gas boiler:

$$COP_{eq}(t) = p_{el}(t)/p_{gas} \cdot \eta_B \tag{22}$$

The COP of economic equivalence is an important metric representing the COP at which the HP is economically equivalent to the gas boiler. Since the controller tends to minimise the operative cost of the system, the HP will operate only if $COP > COP_{eq}$, otherwise the controller will favour the boiler. Moreover, in the configuration without TES, the system is incapable of exploiting periods when low electricity tariffs apply (4 am - 6 am, Figure 6), since generation and demand cannot be decoupled and the balance between them must be met at every moment.

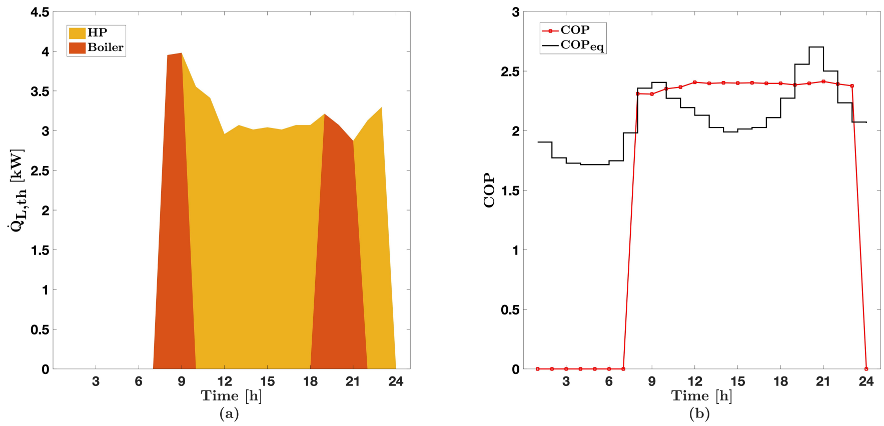

Figure 6: Configuration without TES: Load share between the generators and evolution of COP and COP_{eq} (Day 2).

On the other hand, when a TES is installed, the controller can exploit the available flexibility, thereby taking advantage of lower tariffs (see Figures 7a-7b). Consequently, load-shifting can be observed since the HP is operated to charge the storage tank during the night, when the load demand is zero and the electricity price is lower, reducing the load-share covered by the gas boiler from 33% to 0.3% compared to the configuration without TES. The same behaviour is found for the other days, as per Table 3, which reports the load share between the generators and TES during the considered week.

Finally, it can be observed that, even if the TES allows the most cost-effective load-shifting strategy, the overall energy consumption of the system slightly increases because of the TES thermal losses.

4.2. Impact of DR programmes

The present section analyses the impact on the daily operational cost of different active DR measures, based on the reduction of the daily energy consumption according to specific requests from the grid. To this purpose, the operative (marginal) costs resulting from the variations of the electrical consumption from the baseline identified in the previous section must be determined. All results are based on the solution of the OCP under PBP conditions.

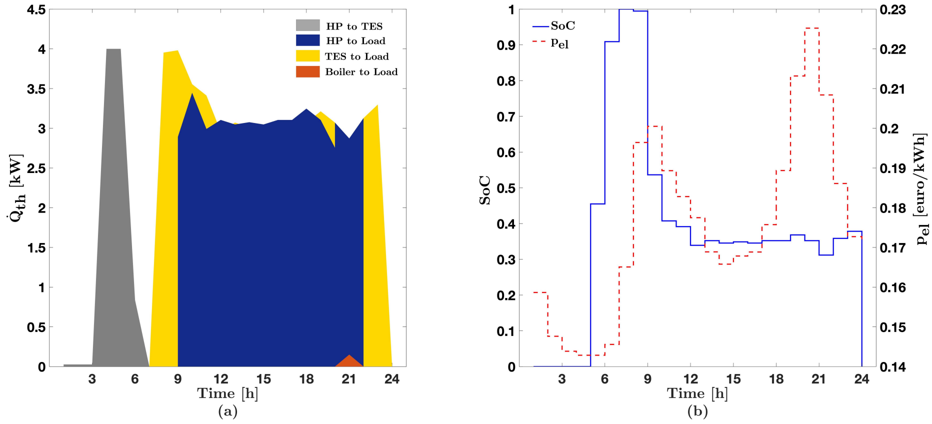

Figure 7: Configuration with TES (Day2): (a) Load share between generators and TES (b) TES State of charge (SoC) and electricity price evolution.

	Boiler [kWh]		**HP_{th} [kWh]**		**HP_{el} [kWh]**		**TES [kWh]**		
	No TES	**TES $0.5m^3$**	**No TES**	**TES $0.5m^3$**	**No TES**	**TES $0.5m^3$**	**No TES**	**TES $0.5m^3$**	**Demand [kWh]**
Day 1	12	0.7	46.6	57.8	19.9	23.1	–	56.9	58.6
Day 2	17	0.6	34.6	52	14.5	20.2	–	51.1	51.7
Day 3	14.3	0	42.2	56.7	17.9	22.3	–	56.5	56.5
Day 4	3.4	0	51.5	55.7	21.8	21.7	–	54.9	54.9
Day 5	12.2	4	51.6	60.6	22.4	24.7	–	59.8	63.8
Day 6	48.5	27	15.9	38.3	6.9	15.6	–	37.4	64.4
Day 7	8.4	0.9	53.6	60	22.7	24.3	–	60.1	61

Table 3: Energy share between generators and TES for each day of the week for configurations without TES and with TES.

Hence, the marginal costs for the provided flexibility are assessed as the ratio of the difference between the new costs and the baseline cost (see Eq. 18) and the reduction in the electrical energy consumption during the DR actions (Eq. 19). At first, a power reduction of the heat pump electric load profile due to the DR equal to 50% and 70% of the reference value ($\alpha = 0.5$ and $\alpha = 0.3$) are considered. Then, a sensitivity analysis on is carried out by varying its value within the range $0.3 - 1$.

Figure 8 refers to the 2^{nd} day of the week considered in previous sections, and it shows the optimal control strategy related to the baseline case, without DR (Figure 8a), and those with DR program implemented (Figures 8b and 8c). The results show an increase in gas boiler usage during the hours in which the DR action is active (at 9am and between 6 pm – 7 pm). At the same time, changes in the use of the storage tank and, consequently, of the heat pump before the DR event are observed. Examining the profile of the state of charge (SoC) of the storage tank, it can be noted that a load-shift occurs just before the start of the DR action: the controller anticipates the DR action by charging the TES and reuse this energy later when the DR action is activated.

Compared to the baseline case (Figure 8a), Figures 8b and Figure 8c show that when the DR is introduced, the HP operates at its maximum power between 4 pm – 5 pm. In this way, a fraction of the thermal energy (34% and 25% for $\alpha = 0.5$ and $\alpha = 0.3$, respectively) can be shifted to the period when the HP has to reduce its power consumption due to the limit imposed by the DR request. It is interesting to note that the same behaviour is not observed for the first DR of the day (at 9 am): in this case, the evolution of the SoC in the baseline case indicates that the storage tank capacity is already at its maximum value ($SoC = 1$) before the start of the DR action. Consequently, the heat pump cannot be operated to anticipate the DR action and, consequently, no modifications in the charging profile occur.

Generally, an energy flexibility event may be followed by a rebound effect. For instance, a DR action aimed at reducing the internal temperature set point is typically followed by a rebound effect due to the energy required to restore the previous temperature set point. However, in the present case study, it is possible to maintain the heat supply as well during the DR event arising from the presence of the TES and the gas boiler, as highlighted in [60]. As a consequence, no rebound effects follow the DR measures, but they result in a higher usage of the heat pump, to charge the TES before that the DR action takes place. It should be pointed out that at the end of the day both the HP operation and the state of charge of the storage are almost the same independently of the applied DR action ($\alpha = 0.5$ or $\alpha = 0.3$). Therefore, each day can be considered as independent by the previous one in terms of DR planning.

Table 4 and Figure 9 assess the effectiveness of the TES in shifting the accumulated energy that must be transferred from the boiler to the heat pump arising from the DR event. Results are presented for a comparative analysis between TES systems with 0.5 m^3 and 0.75 m^3 storage capabilities. For the analysis, different DR actions are considered by varying the value of the parameter α within the range $0.3 - 1$. Referring to Table 4, it can be noted that the load share covered by the boiler decreases as the available storage capacity increases, since the controller is able to exploit the more cost-effective heat pump. Moreover, the load fraction which can be shifted ahead during the day by using the HP before the DR activation depends on the forecast capability as well as on the storage capacity (higher storage capacities lead to higher load shifts and vice-versa). Nevertheless, a saturation of the load-fraction covered by the storage would be expected to occur, if further limitations on the heat pump operation are considered (e.g., when DR occurs over a longer period or for lower α).

The daily cost-deviation and the specific cost of the flexibility provided are reported in Figure 9a. If no TES are installed, the cost-deviation results are proportional to the reduction of the HP electricity consumption. Therefore, the related specific costs remain constant for all α considered. On the other hand, both configurations with TES installed showed a non-linear behaviour of cost-deviation curves. In particular, the cost-deviation increases slowly, as outlined by the values of the related specific costs. This positive effect, is due to the load shift that the controller is capable to operate before the activation of the DR, limiting as consequence the use of the less cost-effective gas boiler. It should be also noted in Figure 9a that the higher values of the cost-deviation (δC_{Flex}) with regard the

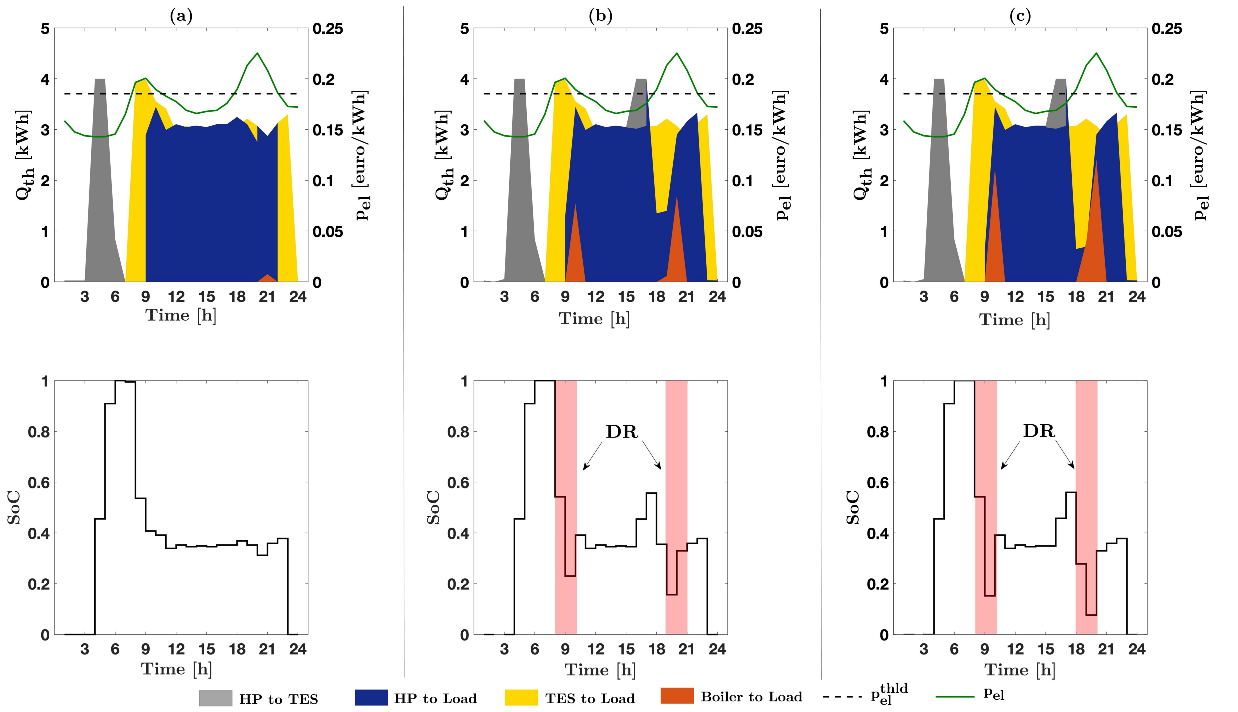

Figure 8: Load share between Boiler and TES and evolution of TES SoC (Day 2): (a) $\alpha = 1$ (no active DR); (b) $\alpha = 0.5$); (c) $\alpha = 0.3$;

configuration with $0.5m^3$ water tank are due to the higher energy reduction performed during the DR (see Figure 9b), and not to a lower efficiency of the process or the TES. In fact, the specific costs decrease as a storage capacity is introduced, highlighting the cost-effectiveness of TES for DR programs.

Finally, it is interesting to note that the configuration with 0.75 m^3 storage presents the same specific costs when a fraction equal to 10% and 20%, respectively, of the baseline electrical energy consumption is reduced as a consequence of DR. Analysing the operation of the generators, compared to the baseline case, it can be noted that the reduction of thermal energy due to DR (0.68 kWh and 1.35 kWh for $\alpha = 0.9$ and $\alpha = 0.8$, respectively), is equal to the energy shifted by operating the HP to pre-charge the storage tank before the DR

	no TES		**TES 0.5 m^3**		**TES 0.75 m^3**	
	Boiler [%]	**HP–TES** [%]	**Boiler** [%]	**HP–TES** [%]	**Boiler** [%]	**HP–TES** [%]
$\alpha = 0.3$	37	63	10	90	3.4	96.6
$\alpha = 0.5$	35.6	64.4	6.5	93.5	2.6	97.4
$\alpha = 1$	33	67	0	100	0	100

Table 4: Load share between the HP/TES and the gas boiler.

request. No variations in the boiler operation are observed, which does not provide any contribution, as in the baseline case (see Table 4 with TES = 0.75 m^3 and $\alpha = 1$). This means that the load demand which cannot be met due to DR limitations can be completely shifted in time, pre-charging the storage tank before the DR request and avoiding in this way to increase the gas boiler production to fulfil the load demand, and consequently the associated specific cost.

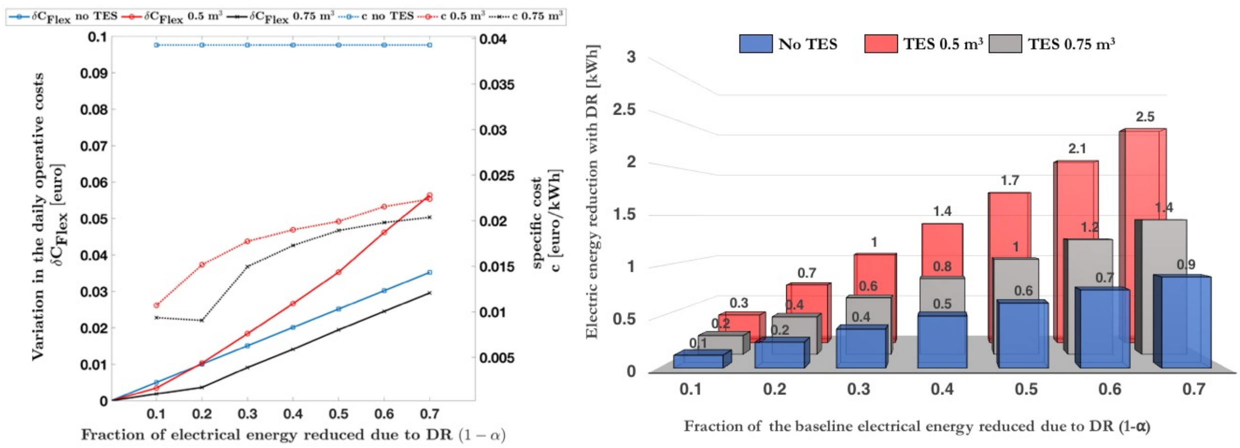

Figure 9: (a) Daily cost and specific costs under different active demand response measures; (b) electrical energy reduced as consequence of DR (Day 2).

4.3. Seasonal assessment of the provided flexibility

Applying the proposed methodology over the whole heating season makes possible to derive maps for each performance indicator (Figures 10a–10c), capable to characterise the energy flexibility offered by the building following demand-response requests from the the grid. To detect those days in which the DR request takes place, Figure 10d shows the evolution over the whole heating season of a DR signal, equal to 1 if one or more DR request take place and zero otherwise.

Results show that the heating season is characterised by two periods of high-demand of flexibility ($\delta = 1$): one across the months of December and January and another one in March (see Figure 10d). It can also be observed that these periods are those in which the highest levels of flexibility are provided ($\delta E_{\mathbf{DR}}$), while low or nil flexibility can be offered at both the beginning and the end of the heating season. Indeed, being these periods characterised by high external temperatures, which lead to a low heating demand, the heat pump power consumption turns out to be low, thus, reducing its power modulation capacity and, consequently, the available flexibility. Moreover, these periods are characterised by a low request of flexibility from the grid, as it shown by the value of the DR signal which is constantly zero across the end of October and the beginning of November. The maximum flexibility potential is achieved in March, when the building can offer a reduction of the energy consumption up to 4.5 kWh, with a cost deviation and an increase in the primary energy consumption of 0.15 € and 3.5 kWh, respectively.

It is important to mention that these maps can be used either by the end-user or by a grid-operator to identify day by day the best DR action to be implemented in accordance with their needs. For instance, an end-user might be interested in identifying the DR action that minimises its cost while preserving the comfort constraint within the building, while a grid-operator might be interested also in those DR actions that minimise the flexibility costs as well as other environmental indicators, such as the primary energy consumption or the total CO_2 emission associated with them.

5. Conclusions

The present work investigated the flexibility potential associated with a building equipped with an optimally controlled hybrid generator (an electrically driven air source heat pump and a gas boiler) under different demand response measures. The impact of thermal energy storage coupled with the heating system and the control strategy of the heat pump unit were also analysed. The main findings can be summarised as follows:

- Impact of the TES: the comparison between the two-studied configurations (without and with TES) demonstrated the cost-effectiveness of installing the TES. The storage tank enables the controller to operate the heat pump by taking advantage of periods during which low electricity tariffs apply, leading to a more cost-effective operation of the heating system. Moreover, this leads not only to a cost-saving up to 8% but also to a reduction of primary energy consumption (and consequently of CO_2 emissions)

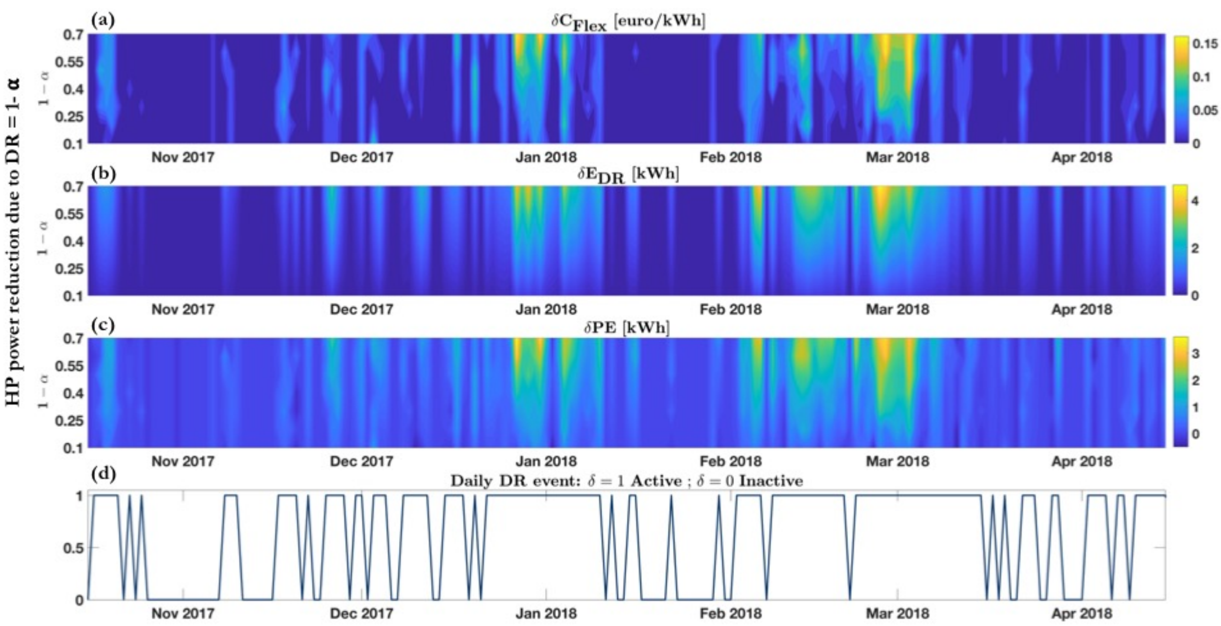

Figure 10: (a-c) Performance maps over the whole heating season and (d) evolution of the DR request.

up to 13% compared to the configuration without TES. Moreover, the TES allows the controller to operate load-shifting throughout the day, thereby limiting the use of the boiler during periods when the COP is lower than the COP of economic equivalence. Critically, the storage capacity and the heat pump size are interdependent: the HP size affects the time needed to charge the storage and consequently the ability to take advantage of the favourable operating periods during the day. On the other hand, the storage capacity limits the amount of energy that can be shifted. The optimal sizing strategy based on these two perspectives should be further investigated.

- Impact of DR programs: the TES allows the controller to operate load-shifting throughout the day, thereby limiting the use of the boiler to meet the load demand that cannot be met by the HP due to the limitations imposed by the DR programme. In this way, a reduction in the specific cost associated with different DR actions between 45% and 75% is observed for the configuration with 0.5 m^3 TES and between 50% and 78% for that with 0.75 m^3 TES. Moreover, the shape of the specific cost curve is affected by the amount of thermal energy that can be shifted by pre-charging the TES before the DR request. If the shifted energy equals the total thermal energy required by the load during the hours where DR is active, the specific cost will remain nearly constant, otherwise it will start to increase proportionally to the fraction of thermal load that cannot be shifted.

- Achievable flexibility: the results showed that the energy flexibility is strictly dependent on the storage capacity and operations which, in turn, are affected by the generator sizing. Further analysis should be carried out to investigate the effects of these parameters on the available flexibility and its marginal cost, as well as to fully characterise the functional relationship between the parameters affecting the cost-curves.

- Performance indicators: the proposed methodology allows the assessment of the energy flexibility potential through its main dimensions by mapping three flexibility indicators: cost–deviation, modulation capacity and efficiency. Those maps can be easily used to identify day by day the best DR action to be implemented and, therefore, they represent useful tools for both building manager and grid-operators.

Attempting to further generalise the presented results, additional simulations with different storage capacities and prediction horizon lengths could be performed, providing conveneint and useful dimensionless correlations for costs and savings, as a function of the provided flexibility by DR actions.

Nomenclature

Acronyms

B Boiler

DR Demand–Response

DSM Demand–Side Management

EMO Electricity Market Operator

HP Heat Pump

ICP Incentive–Based Programs

MPC Model Predictive Control

NLP Non–Linear Programming

nZEB nearly Zero Energy Building

OCP Optimal Control Problem

PBP Price–Based Programs

RES Renewable Energy Systems

SoC State of Charge

TES Thermal Energy Storage

Greek letters

α Percentage of reduction of the electrical power due demand-response action [%]

δ Binary variable

μ_{el} Mean daily electricity price [€$/kWh$]

σ_{el} Standard deviation of the daily electricity price profile

τ Prediction horizon [s]

ε Error in the forecast of the external temperature [^oC]

Symbols

δC_{Flex} Daily flexibility cost–deviation [€]

δE_{DR} Variation of the Heat Pump energy consumption due to demand-response [kWh]

δPE Variation of the Primary Energy consumption due to demand-response [kWh]

ΔT Temperature difference between the storage tank and the surrounding environment [^oC]

$\dot{Q}_{B,th}$ Boiler thermal output $[kW]$

$\dot{Q}_{HP,th}$ Heat Pump thermal output $[kW]$

$\dot{Q}_{L,th}$ Load demand $[kW]$

$\dot{Q}_{TES,loss}$ Storage losses $[kW]$

$\dot{Q}_{TES,th}$ Storage heat rate $[kW]$

η^{II} Heat Pump second-law efficiency

η_B Boiler efficiency

$\mathcal{H}$ Hours in the heating season

ρ_w Water density $[kg/m^3]$

$\widetilde{T}$ External temperature forecast

c Specific cost [€$/kWh$]

C_c Degradation coefficient

C^{α}_{Daily} Daily cost with demand-response [€]

C^{ref}_{Daily} Daily reference cost without demand-response [€]

c_w Specific heat of water $[kJ/kgK]$

COP Heat Pump coefficient of performance

COP_{eq} Heat Pump coefficient of performance of economic equivalence

CR Heat Pump part-load ratio

f_{PL} Part–load correction factor

p_{el} Electricity Price [€$/kWh$]

p_{gas} Gas Price [€$/kWh$]

$P_{HP,el}$ Heat Pump electric power $[kW]$

PE Primary Energy $[kWh]$

t Time $[s]$

$T_{cut-off}$ Heat Pump cut-off temperature $[^oC]$

T_{em} Emission system temperature $[^oC]$

T_{ext} External temperature $[^oC]$

T_{ext}^{des} Design external temperature $[^oC]$

T_{ext}^{off} External temperature at which the heating system is turned–off $[^oC]$

T_H Condenser temperature $[^oC]$

T_L Evaporator temperature $[^oC]$

T_{TES} Storage temperature $[^oC]$

UA_{TES} Storage overall heat transfer coefficient $[kW/K]$

V_{TES} Storage Volume $[m^3]$

Subscripts

B Boiler

DR Scenario with demand-response

FL Full–load

HP Heat Pump

PL Partial–load

TES Thermal Energy Storage

Superscripts

max Maximum

min Minimum

ref Reference scenario

$thld$ Threshold

References

[1] European commission, 2050 energy strategy, online report, https://ec.europa.eu/energy/en/topics/energy-strategy-and-energy-union/2050-energy-strategy, [last accessed: 06/10/2018].

[2] US Energy Information Administration, International energy statistics, 4 March 2018.

[3] A. S. Brouwer, M. Van Den Broek, A. Seebregts, A. Faaij, Impacts of large-scale intermittent renewable energy sources on electricity systems, and how these can be modeled, Renewable and Sustainable Energy Reviews 33 (2014) 443–466.

[4] L. Gelazanskas, K. A. Gamage, Demand side management in smart grid: A review and proposals for future direction, Sustainable Cities and Society 11 (2014) 22 – 30.

[5] L. Schibuola, M. Scarpa, C. Tambani, Demand response management by means of heat pumps controlled via real time pricing, Energy and Buildings 90 (2015) 15–28.
[6] M. H. Albadi, E. F. El-Saadany, A summary of demand response in electricity markets, Electric power systems research 78 (2008) 1989–1996.
[7] M. Starke, D. Letto, N. Alkadi, R. George, B. Johnson, K. Dowling, S. Khan, Demand-side response from industrial loads, in: 2013 NSTI Nanotechnology Conference and Expo, volume 2, p. 46.
[8] M. H. Shoreh, P. Siano, M. Shafie-khah, V. Loia, J. P. Catalão, A survey of industrial applications of demand response, Electric Power Systems Research 141 (2016) 31–49.
[9] M. Carragher, M. De Rosa, A. Kathirgamanathan, D. P. Finn, Investment analysis of gas-turbine combined heat and power systems for commercial buildings under different climatic and market scenarios, Energy Conversion and Management 183 (2019) 35 – 49.
[10] Heat Roadmap Europe 2050, Online report, https://heatroadmap.eu/wp-content/uploads/2018/09/3.1-Profile-of-the-heating-and-cooling-demand-in-the-base-year-in-the-14-MSs-in-the-EU28-2.pdf, [last accessed: 31/05/2019].
[11] European Union, Directive 2010/31/eu of the european parliament and of the council 19 may 2010 on the energy performance of buildings (recast), 2010. In Official Journal of the European Union.
[12] European Union, Directive 2012/27/eu of the european parliament and of the council of 25 october 2012 on energy efficiency, amending directives 2009/125/ec and 2010/30/eu and repealing directives 2004/8/ec and 2006/32/ec, 2012. In Official Journal of the European Union.
[13] European Union, Directive (eu) 2018/844 of the european parliament and of the council of 30 may 2018 amending directive 2010/31/eu on the energy performance of buildings and directive 2012/27/eu on energy efficiency, 2010. In Official Journal of the European Union.
[14] Smart Readiness Indicator for Buildings, https://smartreadinessindicator.eu, [last accessed: 05/04/2019].
[15] M. Miara, D. Günther, Z. L. Leitner, J. Wapler, Simulation of an air-to-water heat pump system to evaluate the impact of demand-side-management measures on efficiency and load-shifting potential, Energy technology 2 (2014) 90–99.
[16] F. D'Ettorre, M. De Rosa, P. Conti, E. Schito, D. Testi, D. P. Finn, Economic assessment of flexibility offered by an optimally controlled hybrid heat pump generator: a case study for residential building, Energy Procedia 148 (2018) 1222–1229.
[17] K. Hedegaard, O. Balyk, Energy system investment model incorporating heat pumps with thermal storage in buildings and buffer tanks, Energy 63 (2013) 356–365.
[18] D. Fischer, T. Wolf, J. Wapler, R. Hollinger, H. Madani, Model-based flexibility assessment of a residential heat pump pool, Energy 118 (2017) 853–864.
[19] A. Arteconi, N. J. Hewitt, F. Polonara, Domestic demand-side management (dsm): Role of heat pumps and thermal energy storage (tes) systems, Applied thermal engineering 51 (2013) 155–165.
[20] F. Ruiz-Calvo, M. De Rosa, P. Monzó, C. Montagud, J. M. Corberán, Coupling short-term (b2g model) and long-term (g-function) models for ground source heat exchanger simulation in trnsys. application in a real installation, Applied Thermal Engineering 102 (2016) 720–732.
[21] D. Dominković, P. Gianniou, M. Münster, A. Heller, C. Rode, Utilizing thermal building mass for storage in district heating systems: Combined building level simulations and system level optimization, Energy 153 (2018) 949–966.
[22] C. Finck, R. Li, R. Kramer, W. Zeiler, Quantifying demand flexibility of power-to-heat and thermal energy storage in the control of building heating systems, Applied Energy 209 (2018) 409–425.
[23] G. Reynders, R. A. Lopes, A. Marszal-Pomianowska, D. Aelenei, J. Martins, D. Saelens, Energy flexible buildings: An evaluation of definitions and quantification methodologies applied to thermal storage, Energy and Buildings (2018).
[24] J. Clauß, C. Finck, P. Vogler-Finck, P. Beagon, Control strategies for building energy systems to unlock demand side flexibility–a review, in: IBPSA Building Simulation 2017, San Francisco, 7-9 August 2017, IBPSA.
[25] A. Stafford, An exploration of load-shifting potential in real in-situ heat-pump/gas-boiler hybrid sys-

tems, Building Services Engineering Research and Technology 38 (2017) 450–460.

[26] F. Oldewurtel, D. Sturzenegger, G. Andersson, M. Morari, R. S. Smith, Towards a standardized building assessment for demand response, in: Decision and Control (CDC), 2013 IEEE 52nd Annual Conference on, IEEE, pp. 7083–7088.

[27] R. De Coninck, L. Helsen, Quantification of flexibility in buildings by cost curves–methodology and application, Applied Energy 162 (2016) 653–665.

[28] M. Ali, A. Alahäivälä, F. Malik, M. Humayun, A. Safdarian, M. Lehtonen, A market-oriented hierarchical framework for residential demand response, International Journal of Electrical Power & Energy Systems 69 (2015) 257–263.

[29] G. Bianchini, M. Casini, A. Vicino, D. Zarrilli, Demand-response in building heating systems: A model predictive control approach, Applied Energy 168 (2016) 159–170.

[30] S. Ø. Jensen, H. Madsen, R. Lopes, R. G. Junker, D. Aelenei, R. Li, S. Metzger, K. B. Lindberg, A. J. Marszal, M. Kummert, et al., Annex 67: Energy flexible buildings-energy flexibility as a key asset in a smart building future (2017).

[31] R. G. Junker, A. G. Azar, R. A. Lopes, K. B. Lindberg, G. Reynders, R. Relan, H. Madsen, Characterizing the energy flexibility of buildings and districts, Applied Energy 225 (2018) 175 – 182.

[32] R. Renaldi, A. Kiprakis, D. Friedrich, An optimisation framework for thermal energy storage integration in a residential heat pump heating system, Applied Energy 186 (2017) 520 – 529. Sustainable Thermal Energy Management (SusTEM2015).

[33] Pallonetto, F., Oxizidis, S., Duignan, R., Neu, O. and Finn, D., "Demand response optimisation of all-electric residential buildings in a dynamic grid environment: Irish case study", 13th Conference of the International Building Performance Simulation Association, BS 2013; Chambery; France (2013) 1616–1623.

[34] F. Pallonetto, M. De Rosa, F. Milano, D. P. Finn, Demand response algorithms for smart-grid ready residential buildings using machine learning models, Applied Energy 239 (2019) 1265 – 1282.

[35] F. Pallonetto, S. Oxizidis, F. Milano, D. Finn, The effect of time-of-use tariffs on the demand response flexibility of an all-electric smart-grid-ready dwelling, Energy and Buildings 128 (2016) 56 – 67.

[36] L. Kreuder, C. Spataru, Assessing demand response with heat pumps for efficient grid operation in smart grids, Sustainable Cities and Society 19 (2015) 136 – 143.

[37] K. Aduda, T. Labeodan, W. Zeiler, G. Boxem, Y. Zhao, Demand side flexibility: Potentials and building performance implications, Sustainable Cities and Society 22 (2016) 146 – 163.

[38] D. Patteeuw, L. Helsen, Combined design and control optimization of residential heating systems in a smart-grid context, Energy and Buildings 133 (2016) 640–657.

[39] D. Fischer, T. R. Toral, K. B. Lindberg, B. Wille-Haussmann, H. Madani, Investigation of thermal storage operation strategies with heat pumps in german multi family houses, Energy Procedia 58 (2014) 137 144.

[40] B. Baeten, F. Rogiers, L. Helsen, Reduction of heat pump induced peak electricity use and required generation capacity through thermal energy storage and demand response, Applied Energy 195 (2017) 184–195.

[41] M. Dongellini, C. Naldi, G. L. Morini, Seasonal performance evaluation of electric air-to-water heat pump systems, Applied Thermal Engineering 90 (2015) 1072–1081.

[42] G. Bagarella, R. Lazzarin, M. Noro, Sizing strategy of on–off and modulating heat pump systems based on annual energy analysis, International journal of refrigeration 65 (2016) 183–193.

[43] European Committee for Standardisation, Standard en 14825: 2013, air conditioners, liquid chilling packages and heat pumps, with electrically driven compressors, for space heating and cooling e testing and rating at part load conditions and calculation of seasonal performance, 2013.

[44] Italian Committee for Standardisation, Standard uni ts 11300 part 4: 2012, energy performance of buildings e part 4: Renewable energy and other generation systems for space heating and domestic hot water production, 2012.

[45] G. P. Henze, C. Felsmann, G. Knabe, Evaluation of optimal control for active and passive building thermal storage, International Journal of Thermal Sciences 43(2) (2004) 173 183.

[46] S. F. Fux, M. J. Benz, L. Guzzella, Economic and environmental aspects of the component sizing for a stand-alone building energy system: A case study, Renewable Energy 55 (2013) 438–447.
[47] D'Ettorre, F., Conti, P., Schito, E. and Testi, D., Model predictive control of a hybrid heat pump system and impact of the prediction horizon on cost-saving potential and optimal storage capacity, Applied Thermal Engineering 148 (2019) 524 – 535.
[48] B. Baeten, F. Rogiers, D. Patteeuw, L. Helsen, Comparison of optimal control formulations for stratified sensible thermal energy storage in space heating applications, The 13th International Conference on Energy Storage (2015).
[49] S. Kalaiselvam, R. Parameshwaran, Thermal energy storage technologies for sustainability: systems design, assessment and applications, Elsevier, 2014.
[50] B. Felten, C. Weber, The value(s) of flexible heat pumps assessment of technical and economic conditions, Applied Energy 228 (2018) 12921319.
[51] L. R. Rodríguez, J. S. Ramos, S. Á. Domínguez, U. Eicker, Contributions of heat pumps to demand response: A case study of a plus-energy dwelling, Applied Energy 214 (2018) 191–204.
[52] European Committee for Standardisation, Standard en 15603: 2008, energy performance of buildings e overall energy use and definition of energy ratings, 2008.
[53] Gazzetta Ufficiale della Repubblica Italiana, Decree of the president of the italian republic no. 412, 26/08/93 and subsequent modifications, 1993.
[54] Comitato Termotecnico Italiano, Documentation available at https://www.cti2000.it (in italian), [Last accessed: 07/10/2018].
[55] G. Bagarella, R. Lazzarin, M. Noro, Annual simulation, energy and economic analysis of hybrid heat pump systems for residential buildings, Applied Thermal Engineering 99 (2016) 485–494.
[56] D. Fischer, K. B. Lindberg, H. Madani, C. Wittwer, Impact of pv and variable prices on optimal system sizing for heat pumps and thermal storage, Energy and Buildings 128 (2016) 723733.
[57] Gestore Mercati Energetici, Online database.www.mercatoelettrico.org/it/statistiche/me/datisintesi.aspx (in italian), [last accessed: 07/10/2018].
[58] M. Kelly, An introduction to trajectory optimization: How to do your own direct collocation, SIAM Review 59 (2017) 849–904.
[59] J. A. E. Andersson, J. Gillis, G. Horn, J. B. Rawlings, M. Diehl, Casadi: a software framework for nonlinear optimization and optimal control, Mathematical Programming Computation (2018).
[60] L. Zhang, N. Good, P. Mancarella, Building-to-grid flexibility: Modelling and assessment metrics for residential demand response from heat pump aggregations, Applied Energy 233 (2019) 709–723.

Mapping the energy flexibility potential of single buildings equipped with optimally-controlled heat pump, gas boilers and thermal storage

Highlights

- The TES allows a cost and primary energy consumption up to 8% and 13% respectively.
- The energy flexibility depends on the TES capacity and the operation control.
- The DR specific cost is reduced between 45% and 75% with TES installed.
- Performance maps can be created to characterise building flexibility potential

Mapping the energy flexibility potential of single buildings equipped with optimally-controlled heat pump, gas boilers and thermal storage

by

Francesco D'Ettorre, Mattia De Rosa, Paolo Conti, Daniele Testi and Donal Finn

Affiliations

Francesco D'Ettorre

- BETTER (Building Energy Technique and Technology Research Group), Department of Energy, Systems, Territory and Constructions Engineering (DESTEC), University of Pisa. Italy

Email: francesco.dettorre@ing.unipi.it

Mattia De Rosa

- School of Mechanical and Materials Engineering. University College Dublin. Belfield, Dublin 4. Ireland
- UCD Energy Institute. University College Dublin. Belfield, Dublin 4. Ireland

Email: mattia.derosa@ucd.ie

Paolo Conti

- BETTER (Building Energy Technique and Technology Research Group), Department of Energy, Systems, Territory and Constructions Engineering (DESTEC), University of Pisa. Italy

Email: paolo.conti@unipi.it

Daniele Testi

- BETTER (Building Energy Technique and Technology Research Group), Department of Energy, Systems, Territory and Constructions Engineering (DESTEC), University of Pisa. Italy

Email: daniele.testi@unipi.it

Donal Finn

- School of Mechanical and Materials Engineering. University College Dublin. Belfield, Dublin 4. Ireland
- UCD Energy Institute. University College Dublin. Belfield, Dublin 4. Ireland

Email: donal.finn@ucd.ie

Corresponding author:

Dr Mattia De Rosa
School of Mechanical and Materials Engineering
UCD Energy Institute
University College Dublin
Belfield, Dublin 4. Ireland.
Emai: mattia.derosa@ucd.ie; mattia.derosa@outlook.com.

Acknowledgments

This work emanated from research conducted with the financial support of Science Foundation Ireland under the SFI Strategic Partnership Programme (Grant Number SFI/15 /SPP/E3125).

The collaboration between the University of Pisa and the University College Dublin was funded by the European Commission through the Erasmus+ program.

Declaration of Interests:

The Authors declare no conflicts of interest